GL-TR-90-0222

Visual Photometric Experiment Data Analysis

Andrew J. Mazzella, Jr.
Kevin P. Larson

RDP Inc.
Waltham Office Center
486 Totten Pond Road
Waltham, MA 02154

30 July 1990

Scientific Report NO. 4

GEOPHYSICS LABORATORY
AIR FORCE SYSTEMS COMMAND
UNITED STATES AIR FORCE
HANSCOM AIR FORCE BASE, MASSACHUSETTS 01731-5000

"This technical report has been reviewed and is approved for publication"

Paul D. LeVan
PAUL D. LEVAN
CONTRACT MANAGER

STEPHAN D. PRICE
BRANCH CHIEF

FOR THE COMMANDER

R Earl Good
R. EARL GOOD
DIVISION DIRECTOR

This report has been reviewed by the ESD Public Affairs Office (PA) and is releasable to the National Technical Information Service (NTIS).

Qualified requestors may obtain additional copies from the Defense Technical Information Center. All others should apply to the National Technical Information Service.

If your address has changed, or if you wish to be removed from the mailing list, or if the addressee is no longer employed by your organization, please notify GL/DAA, Hanscom AFB, MA 01731. This will assist us in maintaining a current mailing list.

Do not return copies of this report unless contractual obligations or notices on a specific document requires that it be returned.

Unclassified
SECURITY CLASSIFICATION OF THIS PAGE

REPORT DOCUMENTATION PAGE

1a. REPORT SECURITY CLASSIFICATION Unclassified	1b. RESTRICTIVE MARKINGS
2a. SECURITY CLASSIFICATION AUTHORITY	3. DISTRIBUTION / AVAILABILITY OF REPORT Approved for public release; distribution unlimited
2b. DECLASSIFICATION / DOWNGRADING SCHEDULE	
4. PERFORMING ORGANIZATION REPORT NUMBER(S)	5. MONITORING ORGANIZATION REPORT NUMBER(S) GL-TR-90-0222
6a. NAME OF PERFORMING ORGANIZATION RDP, Incorporated 6b. OFFICE SYMBOL (If applicable)	7a. NAME OF MONITORING ORGANIZATION Geophysics Laboratory
6c. ADDRESS (City, State, and ZIP Code) 486 Totten Pond Road Waltham, Massachusetts 02154	7b. ADDRESS (City, State, and ZIP Code) Hanscom Air Force Base Massaschusetts 01731-5000
8a. NAME OF FUNDING / SPONSORING ORGANIZATION 8b. OFFICE SYMBOL (If applicable)	9. PROCUREMENT INSTRUMENT IDENTIFICATION NUMBER F19628-87-C-0065
8c. ADDRESS (City, State, and ZIP Code)	10. SOURCE OF FUNDING NUMBERS

PROGRAM ELEMENT NO.	PROJECT NO.	TASK NO.	WORK UNIT ACCESSION NO.
62101F	7670	06	AS

11. TITLE (Include Security Classification)
Visual Photometric Experiment Data Analysis

12. PERSONAL AUTHOR(S)
Mazzella, Andrew J., Jr., Larson, Kevin P.

13a. TYPE OF REPORT	13b. TIME COVERED	14. DATE OF REPORT (Year, Month, Day)	15. PAGE COUNT
Scientific Report #4	FROM 87-Jan-23 TO 90-Jan-31	90-Jul-30	26

16. SUPPLEMENTARY NOTATION

17. COSATI CODES			18. SUBJECT TERMS (Continue on reverse if necessary and identify by block number)
FIELD	GROUP	SUB-GROUP	Visual Radiometer; Zodiacal Light; Star Field Matching;
17	03		
03	01		

19. ABSTRACT (Continue on reverse if necessary and identify by block number)

Data processing and analysis developments for the Visual Photometric Experiment (VIPER) are described, including support for the camera and visual radiometer processing, pre-flight laboratory calibration and development of the star field matching algorithm for the post flight pointing determination.

20. DISTRIBUTION / AVAILABILITY OF ABSTRACT	21. ABSTRACT SECURITY CLASSIFICATION
☒ UNCLASSIFIED/UNLIMITED ☐ SAME AS RPT. ☐ DTIC USERS	Unclassified

22a. NAME OF RESPONSIBLE INDIVIDUAL	22b. TELEPHONE (Include Area Code)	22c. OFFICE SYMBOL
Paul LeVan	(617) 377-4550	OPC

DD FORM 1473, 84 MAR — 83 APR edition may be used until exhausted. All other editions are obsolete.

SECURITY CLASSIFICATION OF THIS PAGE
Unclassified

PREFACE

This report describes the analysis and support provided by the Data Analysis Services group of RDP Incorporated for the development and testing of the VIPER payload, and for the development of the post-flight data processing and analysis software. Other members of this group who have contributed to this effort are Michael Delorey, Peter Dickson, James Hughes, Steven Lacaire, John Palys, and Rahul Rao.

This effort is being performed in conjunction with the research efforts of GL/OPC, for the study of celestial backgrounds, and with the engineering efforts of GL/LCE and their supporting contractors (notably Wentworth Institute of Technology), for the development of GAS Can payloads.

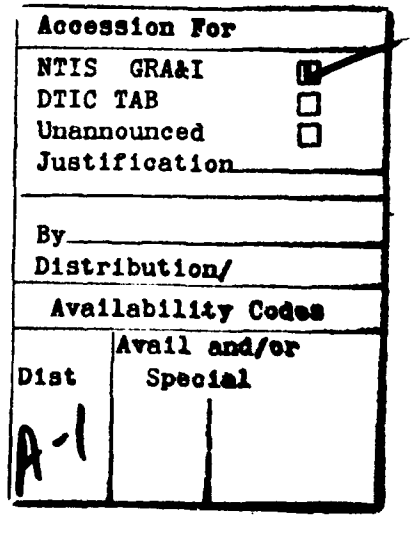

CONTENTS

ILLUSTRATION

Visual Photometric Experiment (VIPER)
Data Analysis

INTRODUCTION

The Visual Photometric Experiment (VIPER) is an instrument package designed for a shuttle-borne Get-Away Special canister (GAS Can). The visual photometer instrument will measure the diffuse zodiacal and galactic emission at standard astronomical wavelengths, using a rotating filter wheel. The precision pointing information will be provided by two sensitive television cameras, an intensified Xybion and a standard Pulnix, incorporated into the instrument package. RDP is developing software to support the pre-flight instrument development and the post-flight data processing and analysis.

The principal efforts have been:
1) the design, evaluation, and development of the pointing determination algorithm, its reference catalogue, and the associated software,
2) development of software for utilization of the video frame acquisition and processing, and
3) support for the laboratory tests of the VIPER instrument.

POINTING DETERMINATION AND STAR FIELD PROCESSING

The design and evaluation of the pointing determination algorithm involved a number of interrelated effects. It was determined that the background levels in each camera pixel due to the galactic and zodiacal backgrounds would be small compared to the brightness of the stars to be selected, but the digitization effects for the 8-bit analog-to-digital converter for the camera images would be significant, imposing a six-magnitude (stellar) dynamic range on the digitized data. The current expectation is that this dynamic range will be from eighth magnitude to second magnitude, for a fully-opened Xybion camera iris, and fifth magnitude to zero magnitude, for a fully-opened Pulnix camera iris. The Xybion range spans the sixth magnitude to third magnitude range, which was determined to be the optimal range for pattern distinctions, providing enough stars to allow a pattern to be determined but not so many as to produce ambiguous matches. For this magnitude range, the Yale Bright Star catalogue appears to provide adequate completeness to be used as a reference for the star pattern matching.

Unfortunately, it appears as though the dynamic range of the Pulnix camera may not be adequate for pattern matching, because there will generally not be enough stars brighter than the fifth magnitude threshold of the Pulnix to establish a pattern. A modification was proposed for the VIPER payload which would alternate the camera for which VHS recording is in effect with every filter change of the visual radiometer (once every 12

seconds), rather than with each complete rotation of the filter wheel (once every 60 seconds). This modification has been incorporated.

For an 8-bit digitization of the TV camera data, a substantial amount of time and storage would be required to digitize every camera frame. However, because the TV frame rate is much more rapid than the rate at which the star fields change, not every frame need be digitized. For a sensor scan rate of one degree per second, produced by the rotation of the Shuttle, an adequate frame digitization rate would be one frame per second. For a scan at the orbital rate (one degree every fifteen seconds), a lower sampling rate can be tolerated. Currently, because of the nature of the VHS playback unit, there is no control over which frames can be selected for digitization. Storage requirements can be minimized by incorporating the first phase of star identification (termed "star discovery") together with the digitization process. In this method, the positions and magnitudes of the stars would be determined from the digitized TV frame and stored in a compact format. The digitized TV frame could then be discarded before the next frame is digitized. The trade-off in this approach is maximum sampling rate (due to the time required to execute the star discovery procedure) versus the storage requirements for the image.

Position determinations appear to be limited in accuracy by the size of the camera pixels and the distortion produced by the sensor scan. For a sensor scan rate of one degree per second, the distortion appears not only as a blur of the individual star images, but also as shifts in relative positions between stars at the leading and trailing edges of the scan, due to the non-instantaneous time to perform the raster sampling of the camera image. The tolerances currently considered for position accuracies of individual stars are of the order of an arc-minute, which is considerably smaller than the one degree diameter of the visual radiometer field of view. The star field matching algorithm is described further in Appendix A.

A number of references relating to pointing or attitude determinations from star fields were obtained through the Defense Technical Information Center, and the most promising of these[1] was reviewed in further detail. Some of these methods are of the same nature as the algorithm described in this report, but without the indexing structure based on star magnitudes, and none of the references obviated the development of the current star field determination process.

---

[1] Schempp, E.P., (1983) Celestial Pattern Recognition Allowing Autonomous Earth-surface or Deep-space Positioning, (Master's thesis) Air Force Institute of Technology, Wright-Patterson AFB, Ohio

The star discovery process was defined as a procedure to extract the pixels associated with star images, cluster the appropriate pixels associated with individual stars, and determine intensities and positions for these stars. The total intensity for a star is based on the sum total intensity of all of the pixels associated with the star image, and the position for the star is the intensity-weighted mean (or centroid) of the positions of all of its associated pixels.

The original acquisition plan for video data was modified by RDP to accommodate the assignment of the OPC laboratory minicomputer to a project at a remote site. The basic structure of the acquisition plan remained unchanged, but the implementation involved a Zenith-248 micro-computer, augmented by a hardware interface (a Data Translation DT2851 Video Frame Grabber) for acquiring and digitizing the video recorder data.

A preliminary examination of the Data Translation DT2851 video frame grabber, acquired by GL, was performed, utilizing the tutorial software associated with the frame grabber. The most significant characteristics of the digitized imaging process were determined, for development in the star identification process during the aspect determination. These include:

- device initialization;
- image acquisition to the device memory;
- display of images from the device memory;
- synthesis of images into the device memory, for the creation of a flat-field coefficient table and for overlay displays;
- accessing images in the device memory, for the star discovery algorithm.

Acquisition of the DTIRIS software library (Data Translation, Inc., Marlborough, Massachusetts), for utilization by FORTRAN data acquisition and display programs, was evaluated and recommended, and this software has been purchased.

A star field simulation (see Figure 1) was created for use in the development of the image acquisition and star discovery processing. A back-illuminated template was viewed by the camera from within a dark enclosure to generate the image, which was then acquired into the DT2851 memory and also displayed on an auxiliary monitor, from which it was photographed for this illustration. A video time code, which appears as a binary intensity code in row 14 of the image, has been incorporated into the recorded video data after this illustration was generated.

The DTIRIS software, in conjunction with the DT2851 frame acquisition hardware, has been incorporated into the frame acquisition and display processing on a Zenith-248, and the preliminary implementation of the star discovery processing has been accomplished.

This has been implemented both as a unified process and also as two distinct, sequential stages (pixel selection, followed later by pixel clustering), to avoid potential timing constraints if "real-time" processing is required. "Real-time" processing may not be an obstacle if slow-speed playback of the video recorder is implemented, or if PC control of the video recorder playback is developed.

The time code extraction from the video images was investigated quantitatively, with the development of software routines for incorporation into the star discovery algorithm and the tabulation of video pixel intensities to verify the bit positions of the time code. A significant problem, which has been addressed and apparently circumvented, is the jitter in the entire synchronization/time code pattern. The magnitude of this jitter is about four to six pixels, which is approximately the number of pixels representing two bits. An algorithm was designed and implemented to determine the amount of the jitter using the synchronization pattern at the beginning of the time code, and then to incorporate this shift into the expected positions for the time code bits. The improvement in the number of correct extracted time codes was significant, with the few remaining incorrect times codes apparently being caused by the uncertainty in the bit spacing in terms of pixels. This uncertainty was evaluated using the tabulation of video pixel intensities to verify the bit positions of the time code, and is being further evaluated by tests on many sets of time code data.

A secondary problem is a time constant associated with the electronics for the bit pattern representation, so that the bit pattern is not sharp, and the intensity levels associated with the zero bits varies considerably, depending on the values of adjacent bits. This problem was used to some advantage for the synchronization position matching, and has otherwise been circumvented by an appropriate selection of the threshold that distinguishes zero-bit values from one-bit values.

The complete Yale Bright Star Catalog and its Supplement[2] were acquired, for development and utilization for the aspect determination process. The catalog was transferred to disk, for reference and further re-formatting, and listings of the data were generated.

Development of the reference catalogues for the star field matching process is nearly completed, pending a firm determination of the actual flight date and the further examination of some entries in the Yale Bright Star Catalog. The

---

[2] Hoffleit, D., and Jaschek, C., (1982) The BRIGHT STAR CATALOGUE, 4th Revised Edition, Yale University Observatory, New Haven, Connecticut

first phase of this process was the extraction of the required parameters from the full Yale Bright Star Catalog into a smaller working catalogue. This working catalogue was used to develop the Index and Proximal catalogues to be used in the star field matching algorithm. Discrepancies between the Yale catalogue and a bright star list from C.W. Allen[3] were noted, and further comparisons are being investigated.

A program was developed to precess the Yale Bright Star Catalog stars from epoch 2000 to the flight epoch, which was initially assigned as 1989.5, but will be revised for the actual flight date when the final reference catalogues are generated. This will allow for the proper association with the NASA shuttle orientation references. The precession processing also accommodates proper motions of the individual stars. Both the precession and proper motion effects can be of the order of arc minutes, which is the same order as the position determination tolerances for star images on the TV cameras. Another program was developed to perform a star coalescence process for the catalogue stars, so that adjacent, unresolvable stars are consolidated into a single entity, with a revised magnitude and weighted mean position.

A discrete representation of the celestial sphere was also developed, for mapping the coverage of the index catalogue being created and for post-flight applications in mapping the coverage from the visual radiometer scans. A map of the preliminary index catalogue was then generated. This map reflects the actual distribution of stars on the celestial sphere, and illustrates the difficulties posed by star field matching for the Pulnix camera, because of the significant number of empty regions, at least for stars brighter than sixth magnitude.

A detailed procedural description for the star field matching algorithm was developed. This description includes the search and comparison algorithms for accessing the reference catalogue, allowance for the position and magnitude measurement errors for the camera field stars and the magnitude variability of some of the catalogue stars, potential cross-referencing to the shuttle ephemeris tape, and the calculation of the transformation between the camera viewing coordinates and celestial coordinates.

The star field matching algorithm was completed in its software implementation, although some parameters, such as the video camera calibrations and relative alignments, and some reference data, such as the shuttle orientation, have yet to be specified in a final form. These quantities have been isolated as much as possible in both the algorithm development and the software

---

[3] Allen, C.W. (1976) Astrophysical Quantities, Revised Third Edition, The Athlone Press, London, England

implementation, to avoid significant changes later. The orientation evaluation for the cameras and visual radiometer, based on the star field identification, is included in this implementation, and is described in Appendix B.

The documentation for the shuttle Post-flight Attitude and Trajectory History (PATH) tape was reviewed, and a minimal set of PATH information was specified. This specification is included in Appendix C.

LABORATORY SUPPORT

Planning and programming have been performed in preparation for the visual radiometer laboratory tests. The revised format for the controller data frame was incorporated into the data acquisition process, and subsequent stages of the data processing were designed, including the format for the time-sequence visual radiometer data base.

Discussions have been conducted regarding the implementation of the calibration technique and the alignment method for the visual radiometer and cameras. Based on these, requirements of the visual radiometer calibration test have been determined, to represent source intensity based on output voltages. Subsidiary effects which must also be evaluated from the calibration process are the variation of the visual radiometer signal response with temperature, and the variation of the LED reference source intensity with temperature.

Qualitative operating criteria were determined for the October 1987 environmental test, influenced partly by the absence of a real-time digital data acquisition, analysis, and display capability at that early phase. Earlier analysis for the sun shutter and filter wheel responses to emergence from eclipse were reviewed, for application to the ambient illumination temporal profiles which would be imposed on the system during the environmental tests.

A strip chart record of a selected segment of the environmental test was evaluated, for a preliminary assessment of the visual radiometer performance at different temperatures. However, the temperature variation over that portion of the test was too small to produce a detectable variation.

The data display sequence for the visual radiometer data has been implemented, encompassing the following stages:

a) data acquisition from the PDP-11 tape onto a VAX;
b) checking the data for valid frame words and time marks;
c) selecting the section of data to be plotted;
d) generating plots on a VAX laser plotter.

The particular data sets being displayed were from the VIPER system test sessions. A program to plot the visual radiometer

filter wheel position as a function of time has also been developed, but still requires the position potentiometer calibration in order to be completed. Further laboratory test data have been received and plotted.

The data acquisition programs were modified to accommodate the revised digital tape format for data transferred from the Sunstrand recorder. A digital tape of the December 23, 1987 laboratory test was generated by a FORTRAN/MACRO program written for the PDP-11 by GL/LC, using a format that is essentially an image of the Sunstrand reproducer output, including the reproducer status words, but with the addition of two header words by the transfer program. The large physical tape blocks generated by this transfer program necessitated the use of special VAX system library subroutines that are foreign to the FORTRAN-77 standard. An earlier digital tape had been generated with smaller physical tape blocks using the PDP-11 system COPY command, but it was found that this system routine introduced its own status words into the midst of the data, based on its internally defined block size.

Preliminary plots of the high-gain and low-gain visual radiometer data and filter wheel positions (in uncalibrated units) were generated. The light-emitting diode (LED) calibration pulses can be observed in the visual radiometer data, and coincide with alternate complete rotations of the filter wheel, but the period between calibration pulses does not appear to be 120 seconds, but rather closer to 128 seconds, and, consequently, the filter wheel rotation period is also different from 60 seconds. This problem was investigated by Wentworth Institute of Technology during the refurbishment of the filter wheel timing electronics, and will be re-examined in future laboratory test data.

The visual radiometer signal from the test data was correlated with the filter position data, in order to evaluate the small modulation observed in the visual radiometer data. Consistent patterns were observed for each individual filter, in spite of the absence of external illumination during the test. This phenomenon will be investigated for future laboratory tests, if it persists.

The phase of the calibration pulse with respect to the filter position was observed to be close to a filter location, rather than at a "blank" (obscured) position of the filter wheel. This problem was investigated by Wentworth Institute of Technology during the payload reassembly, and will be re-examined in future laboratory test data.

Complete plots of the December 1987 test data were impeded by synchronization losses and time word errors in the acquired data. A diagnostic program has been developed to report the times and synchronization words, for both the major and minor frames. This

program may be developed into an interactive program to extract valid data segments for further processing, if no simple criteria for excluding bad data can be developed.

The filter wheel pausing positions were examined for stability and reproducibility, as these are the positions at which either a filter or a "blank" is situated in the field-of-view of the visual radiometer. These are therefore the reference positions for selecting celestial background measurement data, or baseline signal or calibration level data. It should be noted that the totally unobscured region for each filter extends approximately 13° to either side of the filter stop position, and the partially obscured region extends approximately 14° farther. The extent of total obscuration in the blank stops is only approximately 17°. These positions were found to be stable and reproducible to within one counter unit (approximately 0.2°) on either side of the average position. Some unusual variation was found in the counter progression at the "wrap-around" transition from the maximum count to zero, but this is not at one of the pausing positions, and should not present a problem for the data analysis.

The "open", "partially obstructed", and "closed" zones of the filter wheel position indicator were determined. In terms of counter units, the filter wheel cycle is approximately as follows:

Counter Position	Filter Status
0-25	Partially obscured
95	Paused at Filter 1
175-255	Partially obscured
255-355	Totally obscured
355-437	Partially obscured
510	Paused at Filter 2
583-663	Partially obscured
663-753	Totally obscured
753-830	Partially obscured
916	Paused at Filter 3
988-1075	Partially obscured
1075-1166	Totally obscured
1166-1253	Partially obscured
1329	Paused at Filter 4
1405-1500	Partially obscured
1500-1575	Totally obscured
1575-1687	Partially obscured
1758	Paused at Filter 5
1845-1920	Partially obscured
1920-2015	Totally obscured
2015-2048	Partially obscured

The sequence of filters for the filter wheel has been designated as Clear (no filter), R (astronomical Red), V (astronomical

Visible), B (astronomical Blue), and Hα (hydrogen 656.3 nm emission), but the phase of the filter sequence with respect to the filter wheel counter remains to be determined during the calibration testing.

A second-level data acquisition program was developed to extract only the visual radiometer data and associated parameters from the PDP-11 source tape format, eliminating the status words associated with the functioning and monitoring of the experiment controller. The uncalibrated visual radiometer radiance values are separated into two files according to gain levels, and are grouped individually into time-sequenced data blocks according to common positions for the filter wheel and sun shutter. The associated parameters for each data block are:

date;
time;
gain flag (high or low);
filter position;
sun shutter position;
temperature sensor value.

A sample listing of data from the December 1987 laboratory test after conversion to this format is included in Appendix D.

Two items of significance are being evaluated for their effects on the analysis and data processing plan. The need to check the consistency of the camera iris settings has been expressed, and may require two calibration tests separated by a moderately long duration of storage time. The second item is associated with the performance of the original video recorder under simulated flight conditions. Acquisition of a flight-qualified video recorder has been successfully pursued by GL, but the capacity of this alternative recorder is only about two hours of camera data. This will reduce the amount of TV camera data available for pointing determinations from the original design goal of eight hours, and the revised expectation of six hours, so that alternative information from shuttle ephemeris data will have to be processed and analyzed to obtain pointing determinations during the later portions of the mission. (The original design goal of eight hours was revised due to the unavailability of optimal quality long-playing VHS tapes.)

DIGITIZED STAR FIELD SIMULATION

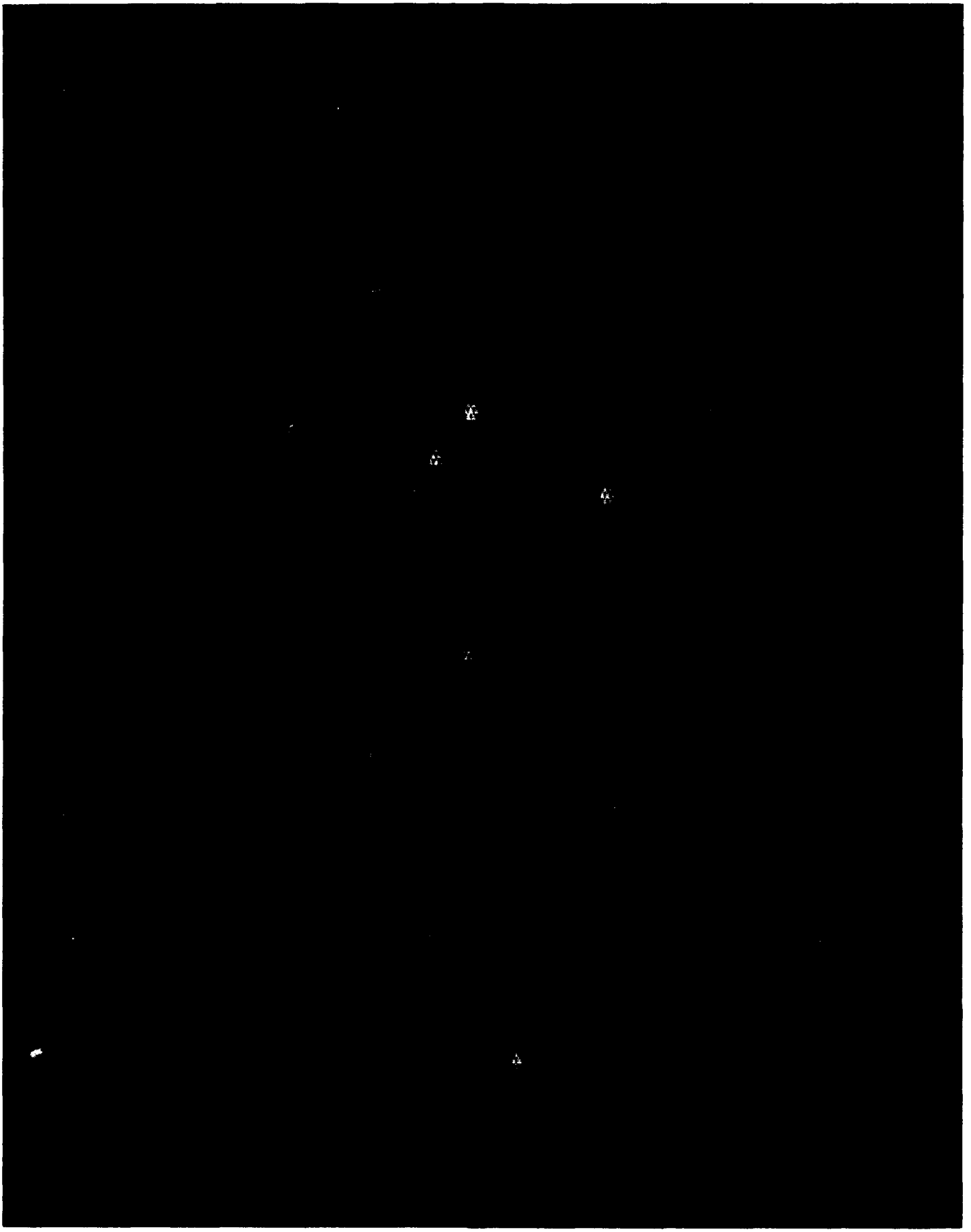

REFERENCES

1. Schempp, E.P., (1983) Celestial Pattern Recognition Allowing Autonomous Earth-surface or Deep-space Positioning, (Master's thesis) Air Force Institute of Technology, Wright-Patterson AFB, Ohio

2. Hoffleit, D., and Jaschek, C., (1982) The BRIGHT STAR CATALOGUE, 4th Revised Edition, Yale University Observatory, New Haven, Connecticut

3. Allen, C.W. (1976) Astrophysical Quantities, Revised Third Edition, The Athlone Press, London, England

4. Cooper, D.H., Parker, K.C., and Torian, J.G. (1985) OPS On-Orbit Postflight Attitude and Trajectory History (PATH) Product Description (JSC-18645), NASA Flight Design and Dynamics Division, Lyndon B. Johnson Space Center, Houston, Texas

Appendix A

VIPER
Pointing Determination Algorithm

The VIPER pointing determination will be based on the data from the two television cameras installed in the instrument package. The Pulnix camera has a 6.72° by 5.04° field of view, with a sensitivity of fifth magnitude, while the Xybion camera has an 11.61° by 7.32° field of view, with a sensitivity of twelfth magnitude, although this will be reduced to eighth magnitude or less by the 8 bit digitization. The two cameras will be alternately recorded to a single VHS recorder. It is the identification of these star fields which will initially provide the pointing determination for the co-aligned visual radiometer.

The algorithm being implemented for the identification of the star fields exploits the magnitude distribution function for visible stars, in that there are relatively few bright stars and many faint stars. Thus, the detection of a star of first magnitude or brighter limits the number of potential viewing regions to 21, while detection of a fourth magnitude star presents approximately 600 potential viewing regions. The number of potential viewing regions is reduced as the magnitude determinations are made with more precision, but the precision of the camera measurements is not expected to be better than one-tenth of a magnitude for a fourth magnitude star. This would reduce the number of potential viewing fields to only about 60, so that further discriminating characteristics must be examined.

The characteristics selected for star field discrimination are the magnitudes of the other stars in the field and their distances from the brightest star in the field. For the Pulnix, there will generally be 1 or 2 other stars, while for the Xybion, there will be about 10 other stars. Thus, star field identifications for the Pulnix will be difficult without auxiliary information, while star field identifications for the Xybion should be accurate.

To facilitate the star field identifications, a set of reference star catalogues has been constructed, based on the Yale Bright Star Catalog. These catalogues will be arranged in a hierarchy, consisting of an index catalogue, and a set of 'proximal' catalogues. The index catalogue was intended to contain at least one reference star for each possible Pulnix field of view, and is arranged in order of increasing magnitudes. Each proximal catalogue will be associated with an entry in the index catalogue and will contain the reference stars potentially visible within the larger Xybion field containing the index star. The angular distances of these stars from the reference star are also

recorded in the proximal catalogue. The index catalogue also contains the positions of each of the stars in celestial coordinates, for use in determining the orientation of the star field and the refined pointing position for the visual radiometer.

The implementation of the star field identification will utilize both the index catalogue and the proximal catalogues. For each observed star field, the brightest star will be matched to an entry in the index catalogue, within the expected magnitude error. The associated proximal catalogue will then be utilized for comparisons of the secondary stars in the observed field, in terms of magnitude and angular distance from the index star. If a reasonable match is found, in terms of the allowable magnitude and position tolerances, then the star field has been identified. The index catalogue can then be accessed to determine the individual star coordinates, for calculation of the orientation of the field. If no match is found for a particular index star, then the next entry in the index catalogue is checked, and its proximal catalogue is investigated if the index entry satisfies the magnitude tolerances for the observed brightest star. Some tolerance for interfering bright objects (planets, satellites) will be incorporated into the implemented algorithm, to minimize the number of fields for which no identification is determined.

When the first star field in a sequence of continuous camera frames has been identified, this information can be used to reduce the search requirements for subsequent star fields in the sequence. Thus, the Xybion star field identifications can be used as auxiliary information for the Pulnix star field observations, reducing or eliminating the potential ambiguity associated with the few stars in the Pulnix field of view.

Appendix B

VIPER Camera/Celestial Coordinate Transformation

Consider the camera field horizontal and vertical coordinates as a local equatorial coordinate system in azimuth (ϕ) and elevation (λ) respectively. The celestial coordinate system is defined by the right ascension angle α (in degrees) and the declination δ. Note that, to retain the same azimuthal convention for the two systems, the camera azimuthal (horizontal) coordinate increases toward the left.

For the coordinate transformation relating the two systems, let

$$\left.\begin{aligned} X &= \cos\lambda \cos\phi \\ Y &= \cos\lambda \sin\phi \\ Z &= \sin\lambda \end{aligned}\right\} \text{camera}$$

$$\left.\begin{aligned} U &= \cos\delta \cos\alpha \\ V &= \cos\delta \sin\alpha \\ W &= \sin\delta \end{aligned}\right\} \text{celestial sphere}$$

Then

$$\begin{bmatrix} U \\ V \\ W \end{bmatrix} = \begin{bmatrix} a_{11} & a_{12} & a_{13} \\ a_{21} & a_{22} & a_{23} \\ a_{31} & a_{32} & a_{33} \end{bmatrix} \begin{bmatrix} X \\ Y \\ Z \end{bmatrix} = \begin{bmatrix} a_{11}X + a_{12}Y + a_{13}Z \\ a_{21}X + a_{22}Y + a_{23}Z \\ a_{31}X + a_{32}Y + a_{33}Z \end{bmatrix}$$

For the stars identified with catalogue entries, let r_{ik} (i = 1, 2, 3) be the celestial coordinates (U, V, W) on the unit sphere associated with each of the N identified stars (k = 1,...,N), and let c_{ik} (i = 1, 2, 3) be the camera coordinates (X, Y, Z) associated with the corresponding star images (k = 1,...,N). The transformation matrix will be determined by minimizing the total squared error between the catalogue coordinates and the transformed camera coordinates:

$$\begin{aligned} E = \sum_k \{ & ([a_{11} c_{1k} + a_{12} c_{2k} + a_{13} c_{3k}] - r_{1k})^2 + \\ & ([a_{21} c_{1k} + a_{22} c_{2k} + a_{23} c_{3k}] - r_{2k})^2 + \\ & ([a_{31} c_{1k} + a_{32} c_{2k} + a_{33} c_{3k}] - r_{3k})^2 \} \end{aligned}$$

$$= \sum_k \sum_{j=1}^{3} ([a_{j1} c_{1k} + a_{j2} c_{2k} + a_{j3} c_{3k}] - r_{jk})^2$$

The derivative conditions on E to produce an extremum are therefore:

$$0 = \frac{\partial E}{\partial a_{\ell 1}} = \sum_k \sum_{j=1}^{3} 2 \left([a_{j1} c_{1k} + a_{j2} c_{2k} + a_{j3} c_{3k}] - r_{jk} \right) c_{1k} \delta_{j\ell}$$

$$= 2 \sum_k \left([a_{\ell 1} c_{1k} + a_{\ell 2} c_{2k} + a_{\ell 3} c_{3k}] - r_{\ell k} \right) c_{1k}$$

$$0 = \frac{\partial E}{\partial a_{\ell 2}} = 2 \sum_k \left([a_{\ell 1} c_{1k} + a_{\ell 2} c_{2k} + a_{\ell 3} c_{3k}] - r_{\ell k} \right) c_{2k}$$

$$0 = \frac{\partial E}{\partial a_{\ell 3}} = 2 \sum_k \left([a_{\ell 1} c_{1k} + a_{\ell 2} c_{2k} + a_{\ell 3} c_{3k}] - r_{\ell k} \right) c_{3k}$$

Thus, the 9 equations for the $a_{\ell m}$ decompose into 3 sets of 3 equations each, for each row of the transformation matrix.

$$\sum_k \left(a_{\ell 1} c_{1k} + a_{\ell 2} c_{2k} + a_{\ell 3} c_{3k} \right) c_{mk} = \sum_k r_{\ell k} c_{mk}$$

or

$$a_{\ell 1} \left(\sum_k c_{1k} c_{mk} \right) + a_{\ell 2} \left(\sum_k c_{2k} c_{mk} \right) + a_{\ell 3} \left(\sum_k c_{3k} c_{mk} \right) = \sum_k r_{\ell k} c_{mk}$$

for $m = 1, 2, 3; \ell = 1, 2, 3.$

Once the transformation matrix is determined, it can be used to transform the center of the camera field coordinates to celestial coordinates, and it can also be used to transform the visual radiometer line-of-sight to celestial coordinates, based on the relative alignment of the visual radiometer and camera.

Euler angles for camera/celestial coordinate transformation.

The camera pointing can be accomplished by the Euler rotations from an initially aligned camera/celestial coordinate system, as follows:

Rotate about Z by ψ, to the right ascension of the line-of-sight;

Rotate about Y' by θ, to the declination of the line-of-sight, so that the camera center is along the line-of-sight;

Rotate about X" by ϕ, so that the camera field is aligned in orientation with the star field.

The inverse transformation is required to transform from the camera field to the celestial coordinates, so:

$$\begin{bmatrix} U \\ V \\ W \end{bmatrix} = \begin{bmatrix} \cos\psi & -\sin\psi & 0 \\ \sin\psi & \cos\psi & 0 \\ 0 & 0 & 1 \end{bmatrix} \begin{bmatrix} \cos\theta & 0 & \sin\theta \\ 0 & 1 & 0 \\ -\sin\theta & 0 & \cos\theta \end{bmatrix} \begin{bmatrix} 1 & 0 & 0 \\ 0 & \cos\phi & -\sin\phi \\ 0 & \sin\phi & \cos\phi \end{bmatrix} \begin{bmatrix} X \\ Y \\ Z \end{bmatrix}$$

$$= \begin{bmatrix} \cos\psi\cos\theta & (\cos\psi\sin\phi\sin\theta - \sin\psi\cos\phi) & (\cos\psi\cos\phi\sin\theta - \sin\psi\sin\phi) \\ \sin\psi\cos\theta & (\sin\psi\sin\phi\sin\theta - \cos\psi\cos\phi) & (\sin\psi\cos\phi\sin\theta - \cos\psi\sin\phi) \\ -\sin\theta & \sin\phi\cos\theta & \cos\theta\cos\theta \end{bmatrix} \begin{bmatrix} X \\ Y \\ Z \end{bmatrix}$$

where

$\theta = -\delta$ (declination)
$\psi = \alpha$ (right ascension angle)
$\phi =$ orientation angle.

Based on the transformation matrix elements:

$\theta = \arcsin(a_{31})$
$\psi = \arctan2(a_{21}, a_{11})$
$\phi = \arctan2(a_{32}, a_{33})$

Appendix C

PATH Data Items for VIPER Pointing

This is the minimal PATH data variable set for utilization with the VIPER pointing determination. The minimally required sampling rate is 0.5 Hz, for at least those periods for which the visual radiometer is recording data. The variable names are those used in the document OPS On-Orbit Postflight Attitude and Trajectory History (PATH) Product Description[4].

ORBIT
Orbit Number

SGMTY\SGMTMO\SGMTD\SGMTH\SGMTM\SGMTS
Greenwich Mean Time (Orbiter): year, month, day, hour, minute, second

GMTY\GMTMO\GMTD\GMTH\GMTM\GMTS
Greenwich Mean Time (Mission Control): year, month, day, hour, minute, second

XTR\YTR\ZTR\XDTR\YDTR\ZDTR
Position\velocity state vector - orbiter: Aries true-of-date Cartesian coordinates (km; km/sec)

INCTR\NODTR
Orbital elements, inclination (degrees) and right ascension of ascending node (degrees) - orbiter: Aries true-of-date coordinates

SUNF
Sunrise (1)/sunset (0) flag

AF
Attitude flag: 0 = telemetry; 1 = interpolation; 2 = attitude timeline (inertial hold); 3 = attitude timeline (solar inertial); 4 = attitude timeline (local vertical/local horizontal); 5 = attitude timeline (rotor); 6 = default attitude (Aries 1950 axes)

ALPHU\BETAU\PHIG
Euler angles for aligning orbiter axes to UVW axes: yaw, pitch, roll (degrees)

---

[4] Cooper, D.H., Parker, K.C., and Torian, J.G. (1985) OPS On-Orbit Postflight Attitude and Trajectory History (PATH) Product Description (JSC-18645), NASA Flight Design and Dynamics Division, Lyndon B. Johnson Space Center, Houston, Texas

TDOTB
Total angular attitude rate: Aries mean of 1950 coordinates (deg/sec)

XBYE\YBYE\ZBYE
Earth position unit vector: shuttle body axis coordinates

XTRM\YTRM\ZTRM
Position state vector - moon: Aries true-of-date coordinates (km)

XTRS\YTRS\ZTRS
Position state vector - sun: Aries true-of-date coordinates (km)

Appendix D

Visual Radiometer Data in Extracted Block Format
December 1987 Laboratory Test

-Header Format-

YYMMDD	TIME	GX	FIPOS	SHPOS	TMP	BSZ
871223	37606.26	1	1126	627	136	10
1454	1402		1435	1418		1483
1472	1382		1497	1426		1453
871223	37606.36	1	1126	629	136	10
1409	1391		1394	1344		1373
1380	1390		1376	1357		1412
871223	37606.46	1	1126	631	136	10
1369	1399		1395	1356		1380
1347	1390		1372	1372		1392
871223	37606.57	1	1125	626	136	10
1531	1382		1436	1430		1394
1468	1437		1383	1443		1464
871223	37606.67	1	1127	629	136	10
1418	1416		1413	1367		1402
1410	1358		1388	1388		1415
871223	37606.77	1	1126	631	136	10
1393	1344		1289	1374		1359
1331	1397		1373	1260		1031
871223	37606.87	1	1126	628	136	20
1462	1405		1399	1484		1011
1404	1400		1378	1440		1340
1404	1369		1400	1421		1436
1389	1422		1414	1414		1414
871223	37607.07	1	1126	631	136	10
1398	1367		1378	1412		1380
1429	1502		1393	1412		1446
871223	37607.18	1	1126	628	135	10
1392	1415		1354	1392		1401
1405	1395		1416	1442		1392
871223	37607.25	1	1127	625	135	10
1418	1382		1382	1417		1392
1423	1382		1403	1462		1392

```
871223  37607.35  1  1126   628 135  10
    1420    1391    1444    1436    1459
    1382    1372    1371    1411    1377

871223  37607.45  1  1126   631 135  10
    1417    1483    1482    1436    1404
    1424    1382    1399    1388    1415

871223  37607.55  1  1126   627 135  10
    1442    1391    1415    1432    1429
    1420    1431    1373    1369    1407

871223  37607.66  1  1125   630 135  10
    1381    1484    1442    1419    1459
    1464    1433    1457    1355    1422

871223  37607.76  1  1125   628 135  10
    1464    1385    1432    1411    1332
    1415    1424    1409    1456    1344

871223  37607.86  1  1126   627 135  10
    1420    1528    1527    1409    1355
    1428    1443    1392    1399    1414

871223  37607.96  1  1125   631 135  10
    1441    1412    1376    1425    1382
    1404    1428    1455    1411    1388

871223  37608.06  1  1125   628 135  10
    1461    1444    1390    1471    1443
    1450    1448    1496    1468    1305

871223  37608.16  1  1126   628 136  10
    1422    1385    1432    1405    1463
    1436    1458    1484    1441    1458

871223  37608.25  1  1127   630 136  10
    1478    1385    1487    1436    1376
    1441    1436    1392    1428    1332

871223  37608.35  1  1126   630 136  10
    1418    1432    1411    1432    1394
    1396    1446    1424    1452    1415
```

YYMMDD = Year (87), Month (12), Day (23)
TIME = Time-of-day (Universal Time) in seconds
GX = Radiometer gain level (0 = low, 1 = high)
FIPOS = Filter wheel position counter
SHPOS = Sun shutter position counter
TMP = Temperature sensor count value
BSZ = Visual radiometer data block size (10 - 100)